

ELASTIC PROTON AND NEUTRON CROSS SECTIONS DERIVED
FROM A MICROSCOPIC OPTICAL MODEL POTENTIAL

A. LEJEUNE,

Université de Liège, Physique Nucléaire Théorique,
Institut de Physique au Sart Tilman, Bâtiment B.5,
B-4000 LIEGE 1, Belgique

1. Introduction

The analysis of experimental p and n elastic cross-sections performed with a phenomenological optical model potential (OMP) has given quite impressive results. It is now considered as a classical tool in nuclear physics. However, this OMP is not free of ambiguities. Therefore, one purpose of a theoretical approach may be to give a guide line to phenomenology and to reduce these ambiguities. Moreover, the success of the OMP leads to the important question : why does the OMP work so well ? Those points have suggested a theoretical approach of the OMP. This is the aim of the work done at the University of Liège in collaboration with J.-P. Jeukenne and C. Mahaux during the last years. The detailed informations about this work can be found in Refs. ¹⁻²). The present paper extends up the communication published in Ref. ³).

Let us simply say that our theoretical approach first involves many body techniques to derive the mass operator in nuclear matter from a realistic N-N interaction. As a second step, we use the local density approximation (LDA) to apply our nuclear matter results to finite nuclei. Furthermore, since the microscopic analysis also require a knowledge of the structure of the target nuclei, i.e. the proton and the neutron density distributions, comparison with experimental data enables us to get informations on these features.

In Section 2, we briefly outline the formalism. The numerical results are discussed and conclusions are drawn in Section 3.

2. Definitions and formulae

2.a. Infinite medium

The fundamental function considered in our many body approach is the mass operator $M(\vec{r}, \vec{r}', E)$, for which the Dyson equation

$$G = G^0 + G^0 M G \quad (1)$$

establishes a connection with the Green's functions G and G^0 of the interacting and free particle systems respectively.

Bell and Squires showed⁴⁾ that $M(\vec{r}, \vec{r}', E)$ and the OMP satisfy the same Schrödinger equation

$$-\frac{\hbar^2}{2m} \nabla_{\vec{r}}^2 \psi_E(\vec{r}) + \int d^3r' M(\vec{r}, \vec{r}', E) \psi_E(\vec{r}') = E \psi_E(\vec{r}). \quad (2)$$

This identification enables us to evaluate the OMP by means of the many body theory for M .

In an uniform medium, the OMP is local, density and energy dependent. Performing a Fourier transform on \vec{r} , the OMP is defined "on the energy shell" and written as

$$M_{\rho}(E) = -\gamma_{\rho}(E) - iW_{\rho}(E). \quad (3)$$

Extended study¹⁾ of $M_{\rho}(E)$ evaluated the isovector component and the correction due to the Coulomb field.

Our use of a hard core realistic nucleon nucleon interaction, lead us to extend Brueckner's method for the binding energy of nuclear matter. In this way, the mass operator is expanded in a power series of the density ρ . All the detailed informations can be found in Refs. ^{1,2)}, where the calculations have been limited to the first leading term of this expansion known as the Brueckner Hartree-Fock approximation. Some of the higher order terms can be evaluated but the others are very difficult to calculate.

2.b. Finite nuclei

The simplest approximation for constructing the OMP

in a finite nucleus from the nuclear matter OMP $M_\rho(E)$ is given by the following LDA

$$M_{k_F(r)}(E) \rightarrow M_{\rho(r)}(E) \rightarrow M_E(r). \quad (4)$$

It is well known however that such an LDA is not convenient to describe the surface effects. The Hartree approximation (let us drop the exchange term) can enlighten this feature.

For a central interaction $v(r)$, the Hartree approximation gives, in an infinite medium of constant density ρ

$$\tilde{M}_H = \rho \int v(r') d^3r'. \quad (5)$$

The simple LDA (4) will provide the corresponding potential in a finite nucleus,

$$\tilde{M}_H(r) = \rho(r) \int v(r') d^3r' \quad (6)$$

but the exact Hartree expression in a finite system is given by the expression

$$M_H(r) = \int \rho(r') v(|\vec{r}-\vec{r}'|) d^3r'. \quad (7)$$

So, expressions (6) and (7) will be identical only if the medium is uniform or if the interaction has a zero range. Approximation (4) is thus not convenient to describe the surface region of the nucleus. Hence, we introduced a range t of the *effective* interaction ($M_\rho(E)/\rho$) and used an "improved" LDA like

$$\tilde{M}_E(r) = (t\sqrt{\pi})^{-3} \int \left(\frac{M_E(r')}{\rho(r')} \right) \exp\left(-\frac{|\vec{r}-\vec{r}'|^2}{t^2}\right) \rho(r') d^3r', \quad (8)$$

or, equivalently

$$\tilde{V}_E(r) = (t_{re}\sqrt{\pi})^{-3} \int v_E(r') \exp\left(-\frac{|\vec{r}-\vec{r}'|^2}{t_{re}^2}\right) d^3r', \quad (9a)$$

and

$$\tilde{w}_E(r) = (t_{im} \sqrt{\pi})^{-3} \int w_E(r') \exp\left(-\frac{|\vec{r}-\vec{r}'|^2}{t_{im}^2}\right) d^3r' \quad (9b)$$

for the real and the imaginary parts respectively.

The ranges t_{re} and t_{im} are the only phenomenological parameters in our calculations. They are adjusted to fit the volume integrals and the RMS radii of the phenomenological OMP, and can be different for the real and the imaginary parts.

For the proton and neutron density distributions of the targets, we tested various available density distributions. We finally adopted the ones which gave the lowest χ^2 , i.e. the point like nucleon mass distribution of Malaguti and Hodgson⁵⁾ for the nuclei up to ^{40}Ca and the Negele's formula⁶⁾ for the heavier nuclei.

However, the microscopic approach does not yet include a spin orbit potential. The latter was taken from phenomenological analyses. It is not important as far as the polarizations are disregarded.

3. Results and discussion

Using our theoretical OMP, we evaluate different quantities and compare them to the phenomenological or experimental data. The volume integrals and RMS radii of the real and imaginary parts of the OMP appear to be the most significant features of the potential. Direct calculations of elastic scattering cross-section provide informations on the shape of the OMP and on the accuracy of matter density distributions.

Let us first look at the volume integrals and the RMS radii. In the frame of a leptodermous model, Myers⁷⁾ showed that the volume integrals do not change when going from a simple LDA (Eq. (4)) to the improved LDA (Eqs. (9)) but the RMS radii are increased by an amount proportional to t_{re}^2 or t_{im}^2 . This property suggested our choice of an improved LDA which gives better agreement between empirical and calculated RMS radii.

In Fig. 1, we show the energy dependence of the quan-

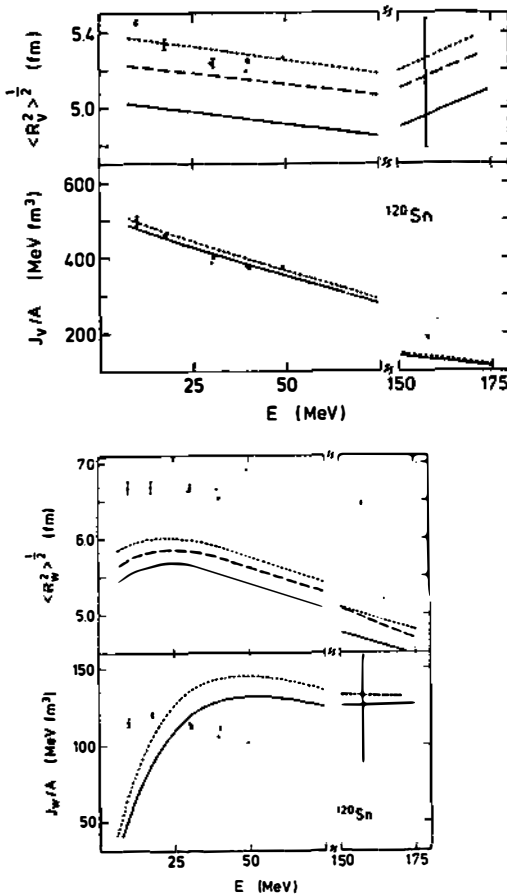


Fig. 1 - The dots represents the empirical values of the root mean square radius and of the volume integral per nucleon of the real and imaginary part of the proton OMP of ^{120}Sn . The compilations are taken from Perey and Perey⁹). The full and long dashed curves represent the result of the LDA (Eq. (4)) and of the improved LDA (Eq. (9)) respectively. The short dashes correspond to the existence of a neutron-rich skin.

ties J_V/A , $\langle R_V^2 \rangle^{1/2}$, J_W/A and $\langle R_W^2 \rangle^{1/2}$ in the case of protons elastically scattered by ^{120}Sn . We observe a good agreement between theory and experiment for the real part. As concern the imaginary part, the J_W/A is a little bit too large and the improved LDA does not provide a sufficiently large RMS radius.

Figure 2 shows a comparison between J_W/A calculated at four energies and a recent phenomenological compilation⁸) of proton OMP in the energy ranges $E_p > 25$ MeV (upper part) and $E_p < 25$ MeV (lower part). The general trend of

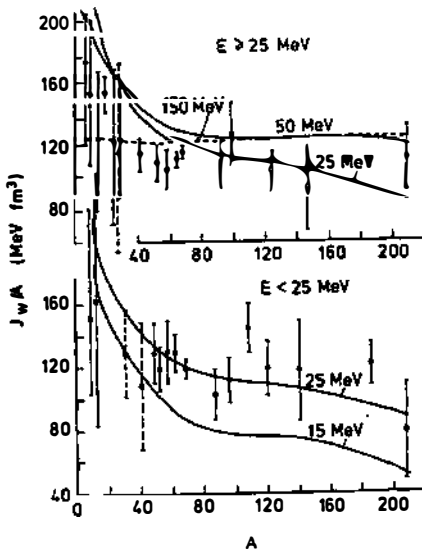


Fig. 2 - Compilation⁸⁾ of empirical values of J_W/A for protons on a wide range of nuclei. The theoretical curves are calculated from the LDA (Eq. (4)).

J_W/A is in nice agreement except for light nuclei. The ranges $t_{re} = t_{im} = 1.2$ fm are used in all the calculations.

We also investigated proton and neutron elastic cross section. Calculations were carried out for a series of nuclei, from ^{12}C to ^{209}Bi . The energy range 10-70 MeV was studied for proton scattering and 1-15 MeV for neutron scattering; these limits are well within those accepted for our model which should be justified up to 180 MeV. The selected density distributions have been quoted above but a neutron skin was found to improve the results for heavy nuclei.

Figures 3-7 show a selection of experimental ρ and n scattering data (full dots) by different targets at various energies. The full curves represent the theoretical cross sections derived from expressions (9). The difference between the half density radii of the neutron and of the proton distributions is taken equal to 0.13 fm for ^{120}Sn , ^{208}Pb and ^{209}Bi . On the average, the results are quite encouraging for a microscopic approach with the ranges t_{re} and t_{im} as only adjustable parameters.

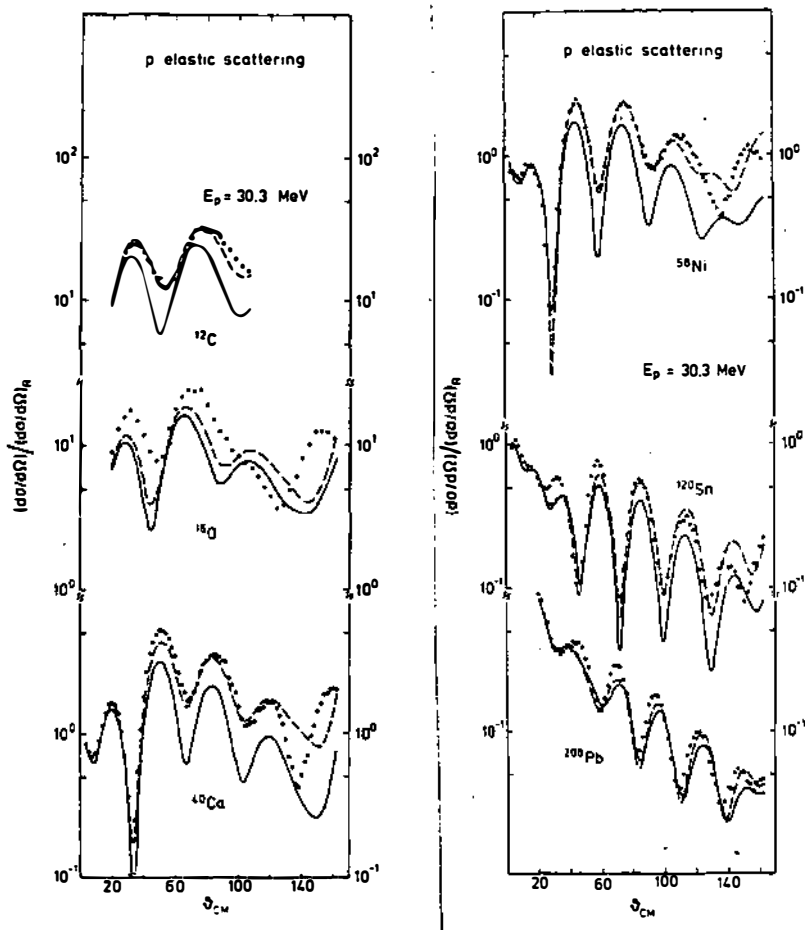


Fig. 3-4 - Differential elastic scattering cross sections for 30.3 protons on various nuclei¹⁰). The full curves are derived from the theoretical OMP (Eq. (9)), the dashed curves from the renormalized OMP.

To improve our theoretical $d\sigma/d\Omega$, we fitted our numerical OMP by a Saxon-Wood (SW) form and a SW plus derivative of SW for the real and imaginary part respectively and we allowed variations of the diffuseness. However, the fits of the $d\sigma/d\Omega$ were not substantially improved. We then renorma-

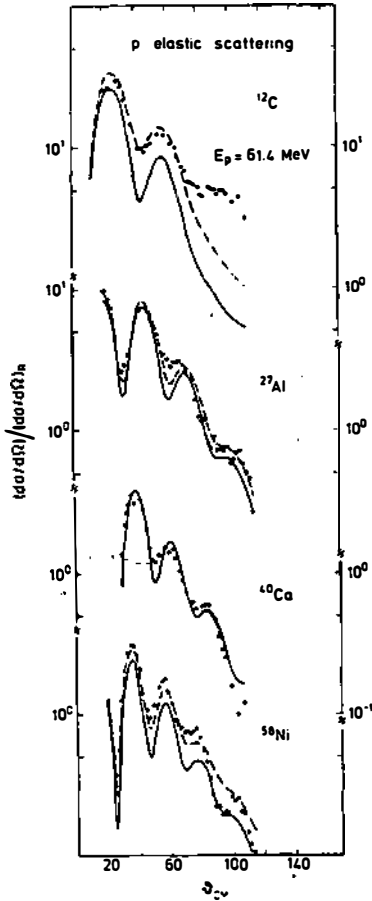


Fig. 5 - Same as Fig. 3 but for 61.4 MeV protons scattering¹⁾.

lized the strengths of $\tilde{V}_E(r)$ and $\tilde{W}_E(r)$. This brought a nice agreement and the results are represented by the dashed curves on Figures 3-7. The corresponding renormalization factors for the strengths are summarized in Table 1.

The most striking results are the following. The real parts of the theoretical OMP have nearly the right magnitude but the imaginary parts are too strong. We observe also a better agreement with higher energies and heavier nuclei. This is in accordance with the study of volume integrals²⁾.

The reasons why the strength of $\tilde{W}_E(r)$ is too large could be ;

i) the selected (for a question of data) targets are at or near closed shells and have then unusually low densities of compound states and high reaction thresholds. This can

be confirmed by the good trend of J_W/A displayed in Fig. 2 through the wide range of nuclei.

ii) we did not include any centre of mass correction ; in particular, the LDA includes a spurious absorptive part which corresponds to the channels where the C.M. of the target is excited.

iii) the higher order terms in the Brueckner expansion might reduce the strength of the imaginary parts.

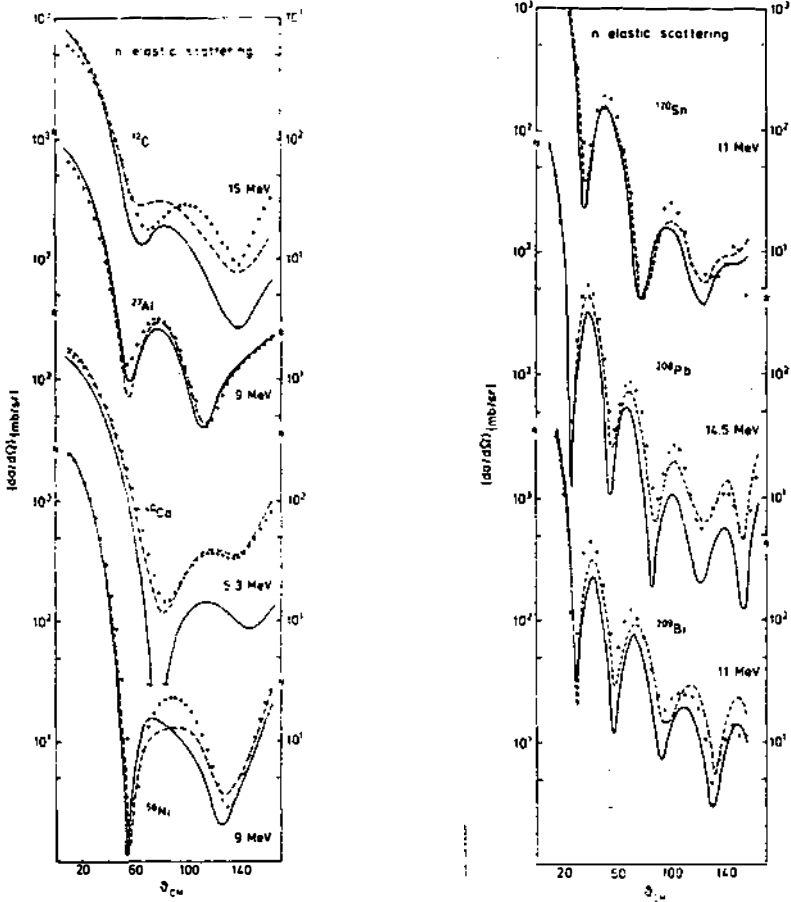


Fig. 6-7 - Same as Fig. 3 but for n scattering¹²⁾.

This microscopic approach to the OMP gives, at first sight, encouraging results. Improvements such as a theoretical evaluation of the spin orbit potential, of the higher order terms and of C.M. corrections should be introduced. Some of these problems are now being studied.

Table 1

Renormalization factors for p and n elastic scattering

Target	Incident Nucleon	E _{lab} (MeV)	Renormalization Factors	
			V	W
¹² C	p	30.3	0.932	0.598
¹⁶ O	p	30.3	0.972	0.818
⁴⁰ Ca	p	30.3	0.992	0.722
⁵⁸ Ni	p	30.3	0.962	0.726
¹²⁰ Sn	p	30.3	1.007	0.822
²⁰⁸ Pb	p	30.3	1.027	0.965
¹² C	p	61.4	1.104	0.704
²⁷ Al	p	61.4	1.002	0.727
⁴⁰ Ca	p	61.4	1.006	1.014
⁵⁸ Ni	p	61.4	1.021	0.845
¹² C	n	15.0	1.027	0.625
²⁷ Al	n	9.0	0.964	0.971
⁴⁰ Ca	n	5.3	0.991	0.379
⁵⁸ Ni	n	9.0	0.968	0.878
¹²⁰ Sn	n	11.0	0.973	0.866
²⁰⁸ Pb	n	14.5	0.976	0.681
²⁰⁹ Bi	n	11.0	0.960	0.722

References

- 1) J.-P. Jeukenne, A. Lejeune and C. Mahaux, Phys.Rep. 25C(1976) 83; Phys.Rev. C10(1974)1331; idem, C15(1977)10.
- 2) J.-P. Jeukenne, A. Lejeune and C. Mahaux, Phys.Rev. C16(1977) 80.
- 3) A. Lejeune, Fizika 9, Suppl. 2 (1977)52.
- 4) J.S. Bell and E.J. Squires, Phys.Rev.Lett. 3(1959)96.
- 5) F. Malaguti and P.E. Hodgson, Nucl.Phys. A215(1973)243 ; Nucl. Phys. A257(1976)37.

- 6) J.W. Negele, Phys.Rev. C1(1970)1260.
- 7) W.D. Myers, Nucl.Phys. A204(1973)465.
- 8) P.E. Hodgson, Phys.Lett. 65B(1976)331.
- 9) C.M. Perey and F.G. Perey, At.Data Nucl. Data Tables 17
(1976)1.
- 10) B.W. Ridley and J.F. Turner, Nucl.Phys. 58(1964)497.
- 11) C.B. Fulner, J.B. Bell, A. Scott and M.L. Whiten, Phys.Rev.
181(1969)1565.
- 12) D. Spaargaren and C.C. Jonker, Nucl.Phys. A161(1971)354 ;
J.D. Reber and J.D. Brandenberger, Phys.Rev. 163(1967)1077 ;
D.E. Velkey et al., Phys.Rev. C9(1974)2181 ;
J.C. Ferrer, J.D. Carlson and J. Rapaport, Nucl.Phys. A275
(1977)325 ;
F.G. Perey and B. Buck, Nucl.Phys. 32(1962)353.

DISCUSSION

K. Dietrich: For the scattering of nucleons by ^{208}Pb you found that the radius of the imaginary part of the optical potential was larger than the one of the real part. Is this a general phenomenon for all target nuclei and would you expect a similar result for heavy ion reactions?

A. Lejeune: Yes, it is a general phenomenon for all the nuclei and I think that it will be the same for heavy ion reactions. I believe that the Pauli principle is responsible for such an effect.

J. Németh: 1. Did you take into account the starting energy correction in the LDA? It can be important for small E .

2. Is the range t independent of the size of the nucleus?

A. Lejeune: No, we did not take into account any starting energy correction in the LDA. As for the range t , you can adjust it from one nucleus to another in order to get good agreement with the J/A and the RMS radii. But, if you consider the quantity $V_E(r)/\rho(r)$ as an "effective interaction", then the range t must be independent of the size of the nucleus.